JOURNAL OF VIROLOGY, Nov. 2004, p. 12416–12427 Vol. 78, No. 22
0022-538X/04/$08.00+0 DOI: 10.1128/JVI.78.22.12416–12427.2004

Inhibition of Interferon-Mediated Antiviral Activity by Murine Gammaherpesvirus 68 Latency-Associated M2 Protein

Xiaozhen Liang, Young C. Shin, Robert E. Means, and Jae U. Jung*

Department of Microbiology and Molecular Genetics and Tumor Virology Division, New England Primate Research Center, Harvard Medical School, Southborough, Massachusetts

Received 15 April 2004/Accepted 29 June 2004

Upon viral infection, the major defense mounted by the host immune system is the activation of the interferon (IFN)-mediated antiviral pathway. In order to complete their life cycle, viruses that are obligatory intracellular parasites must modulate the host IFN-mediated immune response. Murine gammaherpesvirus 68 (γHV68) infects a wide range of cell types and establishes latent infections in mice. Here we demonstrate that the γHV68 latency-associated M2 protein has a cell-type-dependent localization pattern: M2 is present in the cytoplasm and plasma membrane in lymphocytes, whereas it is present primarily in the nucleus in epithelial and fibroblast cells. A mutational analysis indicated that the internal positively charged amino acids of M2 are required for its nuclear localization in fibroblasts. Purification of the M2 complex showed that M2 specifically interacts with the cellular p32 acidic protein through its central positively charged region and that this interaction recruits the cellular p32 protein to the nucleus in fibroblasts. Regardless of its localization, M2 expression effectively induced the downregulation of STAT1 and/or STAT2 in both A20 B lymphocytes and NIH 3T3 fibroblasts, resulting in the inhibition of IFN-α/β- and IFN-γ-mediated transcriptional activation. Finally, the M2 interaction with the p32 protein appeared to contribute to its ability to inhibit IFN-mediated transcriptional activation. These results indicate that γHV68 harbors a latency-associated M2 gene that antagonizes IFN-mediated host innate immunity and thus could play an important role in the establishment and maintenance of viral latency in infected animals.

Herpesviruses persist in their hosts through their ability to establish latent infections and to periodically reactivate to produce infectious virus. To do this, herpesviruses antagonize host immune responses through numerous mechanisms. In particular, gammaherpesviruses can establish lifelong latency within lymphocytes and are associated with the development of lymphomas and other cancers (54). Murine gammaherpesvirus 68 (γHV68) is closely related to primate gammaherpesviruses, herpesvirus saimiri (HVS), rhesus rhadinovirus, Epstein-Barr virus (EBV), and Kaposi's sarcoma-associated herpesvirus (KSHV) (15, 66). The similarity of these viruses, which all cause latent infections in lymphocytes and the development of tumors, indicates that they may share some basic pathogenic mechanisms. γHV68 is a natural pathogen of murid rodents and can infect inbred and outbred strains of mice (3, 4, 5, 49). γHV68 infections in mice result in acute, productive infections of multiple organs, such as the lungs and the spleen. The acute infections are cleared in about 2 to 3 weeks, followed by the establishment of latent infections that persist for life. B cells, macrophages, dendritic cells, and lung epithelial cells are the likely sites of γHV68 latency (16, 55, 57, 59, 60, 70, 71). There is a lack of small-animal models for human gammaherpesviruses such as EBV and KSHV. Thus, γHV68 infections of mice can provide a genetically tractable animal model for the study of gammaherpesvirus pathogenesis and for the development of therapeutic strategies against human herpesviruses (46, 56).

Interferons (IFNs) are a family of cytokines that exhibit diverse biological effects, such as the inhibition of cell growth and protection against viral infection. There are two major subtypes of IFNs, IFN-α/β and IFN-γ. Both subtypes elicit similar yet distinct biological activities. IFN-α/β is a vital signal for the host innate immune system to initiate an antiviral response, provide the first line of innate immune defense against virus infection, and additionally modulate the adaptive immune response (33). IFN-γ, which is produced by activated T cells and natural killer cells, is primarily involved in the regulation of specific immune responses, immune surveillance, and tumor suppression (1, 2). IFNs carry out their responses through activation of the Janus kinase (JAK)-signal transducer and activator of transcription (STAT) signal pathway. Activation of the STAT pathway leads to the formation of two major complexes, namely, γ-activated factor (GAF), which is composed of STAT1 dimers and induced by IFN-γ, and IFN-stimulated gene factor 3 (ISGF3), which consists of STAT1 (p84/91), STAT2 (p113), and a DNA binding protein, p48, and is mainly induced by IFN-α/β. The ISGF3 and GAF complexes translocate to the nucleus, bind to the IFN-stimulated response element (ISRE) and the γ-activated sequence (GAS), respectively, and modulate gene transcription (12, 13, 17, 52, 53).

Most viruses have evolved immune system evasion strategies to protect themselves against host IFN responses, elaborating viral proteins as a counterdefense against the host IFN defenses. Recently, IFN antagonist strategies used by many viruses have been revealed, including the blocking of IFN signaling by the downregulation of JAK-STAT signal molecule basal levels, the suppression of particular molecule modifications, and the prevention of molecule translocation (19, 21, 31, 72). The paramyxovirus family of viruses has been demonstrated to deregulate the STAT signaling pathway to circum-

* Corresponding author. Mailing address: New England Regional Primate Research Center, 1 Pine Hill Dr., Southborough, MA 01772. Phone: (508) 624-8083. Fax: (508) 786-1416. E-mail: jae_jung@hms.harvard.edu.

vent the IFN response (14, 18, 20, 22, 23, 35, 50, 51). Herpesviruses have also been shown to antagonize IFN responses through numerous mechanisms. Herpes simplex virus (HSV) encodes at least two modulators of the IFN response, US11 and infected cell protein 34.5 (ICP34.5). Both viral genes target the double-stranded RNA-dependent protein kinase R pathway to inhibit the IFN response (8). A recent study has also shown that HSV infection occludes IFN signaling at multiple steps, including the inhibition of STAT1 tyrosine phosphorylation and the downregulation of JAK1 and STAT2, and that this activity is partially mediated by the HSV U_L41 gene (11). Furthermore, HSV type 1 (HSV-1)-infected cell protein 0 (ICP0) expression in infected cells has been shown to be critical for determining whether host IFNs repress the HSV-1 genome, suggesting its potential relevance to the establishment of latent HSV-1 infections (26). Various human cytomegalovirus proteins have been demonstrated to induce cellular IFN response genes (32). EBV also blocks the antiviral IFN response through the downregulation of IFN-γ receptor gene expression by BZLF1, an immediate early gene product (45). KSHV has developed a unique mechanism for antagonizing cellular IFN-mediated antiviral activity by incorporating viral homologs to several cellular regulatory genes into its genome. One of the important pirated genes, encoded by the K9 open reading frame (ORF), is a viral homolog of the interferon regulatory factors (vIRF-1), a family of cellular transcription proteins that regulate the expression of genes involved in the pathogen response, immune modulation, and cell proliferation. vIRF-1 has been shown to downregulate IFN- and IRF-mediated transcriptional activation by interacting with CBP/p300 coactivators (37, 39). This indicates that herpesviruses deregulate IFN-mediated innate immunity in various ways to establish and/or maintain persistent infections.

Analyses of γHV68 gene expression have defined four unique open reading frames (M1, M2, M3, and M4) in the left end of the genome. These genes share no homology with those of other gammaherpesviruses (46, 66). Of particular interest is the M2 protein, which has been identified as a latency-associated gene and a target for the host cytotoxic T-lymphocyte response (29). M2 expression has been detected within all latently infected cells in vitro, in lungs within the first month postinfection (29, 42, 62), and in splenocytes in latently infected mice (29, 41, 67). The loss of the M2 gene does not affect the ability of γHV68 to replicate in culture, nor does it affect the acute phase of viral replication in mice after intranasal inoculation (30). However, M2 mutant viruses exhibit a significant decrease in the establishment of latency and reactivation from latency, suggesting that M2 has an important role in latent viral infections (30, 41). Here we demonstrate that the M2 protein has a cell-type-dependent localization and effectively inhibits IFN-mediated signal transduction. Furthermore, we found that M2 interacts with the cellular p32 (also called SF2A-p32) acidic protein (28), and this interaction appears to be involved in the inhibition of IFN-mediated signal transduction. These results indicate that γHV68 may harbor a latently expressed M2 gene that disrupts IFN-mediated host innate immunity and ultimately contributes to the establishment and maintenance of a latent infection.

MATERIALS AND METHODS

Cell culture, cytokine treatment, and transfection. Mouse NIH 3T3 fibroblast cells and mouse A20 B cells were grown in Dulbecco's modified Eagle's medium and RPMI 1460 medium, respectively, supplemented with 10% fetal bovine serum and 1% penicillin-streptomycin (Gibco-BRL). Murine S11 tumor B cells were maintained in RPMI 1460 medium supplemented with 2 mM L-glutamine and 10% fetal bovine serum. Treatments of cells with IFN were performed as indicated, with 1,000 U of IFN-α/β per ml or 5 ng of IFN-γ per ml. Lipofectamine 2000 (Invitrogen) or calcium phosphate (Clontech) was used for M2 expression in NIH 3T3 cells, and electroporation was used for M2 expression in A20 and S11 B cells. A20 and NIH 3T3 cells expressing wild-type (wt) M2 or its mutants were selected and maintained by the presence of puromycin (2 μg/ml).

Plasmids. The M2 coding region was amplified from γHV68 genomic DNA by a PCR with primers 1 (5′-CGCGGATCCATGGCCCCAACACCCCCACAAG-3′) and 2 (5′-GTCGACTCGAGTTAACTTCCTGCAGGGTTAACTTC-3′), which created 5′ BamHI and 3′ XhoI sites (underlined), respectively, for cloning purposes. The amplified DNA fragment was cloned into the BamHI- and XhoI-cut pGEX4T-1 vector (Stratagene) to yield the pGST-M2 fusion construct.

The plasmid pEBG/M2 was generated to express a glutathione *S*-transferase (GST)–M2 fusion protein in mammalian cells. A PCR-amplified M2 fragment with BamHI sites at both ends was cloned into the BamHI cloning site of the pEBG vector to yield the pEBG/M2 construct. Deletions and point mutations in the M2 coding sequence were generated by PCR-based mutagenesis. The mammalian expression construct pEF/M2-AU1, which was used to express the M2 gene, was constructed by use of a 5′ M2-specific primer (untagged) and a 3′ M2-specific primer (with an AU1 epitope tag sequence). All M2 constructs were verified by DNA sequencing.

Protein purification and mass spectrometry. For the identification of M2-binding proteins, [^{35}S]methionine- and [^{35}S]cysteine-labeled mouse A20 B cells (10^7 cells) or 5 liters of A20 cells were resuspended in lysis buffer (0.15 M NaCl, 0.5% Nonidet P-40, and 50 mM HEPES buffer [pH 8.0]) containing protease inhibitors. Precleared lysates were mixed with glutathione beads (Amersham Bioscience) containing GST and the GST-M2 fusion protein for 4 h, and the beads were then washed extensively with lysis buffer. Proteins bound to glutathione beads were eluted and separated by sodium dodecyl sulfate-polyacrylamide gel electrophoresis (SDS-PAGE). Protein bands isolated by SDS-PAGE were analyzed by ion-trap mass spectrometry, and amino acid sequences were determined by tandem mass spectrometry and database searches.

Immunofluorescence. Cells were fixed with 4% paraformaldehyde for 15 min at room temperature and then permeabilized in ice-cold acetone-methanol (1:1) for 20 min at 4°C. After three washes with phosphate-buffered saline (PBS), the samples were blocked with 1% bovine serum albumin in PBS for 30 min at room temperature, subsequently incubated with a 1:500 to 1:2,000 dilution of primary antibody in PBS (plus 1% bovine serum albumin) for 1 h, and then incubated with a 1:2,000 dilution of an Alexa 488- or Alexa 568-conjugated anti-rabbit or anti-mouse antibody (Molecular Probes) for 1 h at room temperature. Topro-3 (Molecular Probes) was used for nuclear staining at a 1:3,000 dilution. Images were obtained by use of a TCSSP confocal microscope (Leica Microsystems).

Reporter gene assays and RNA analysis. Luciferase assays were performed according to the manufacturer's instructions (Promega) by cotransfecting cDNA expression plasmids, a reporter gene, and a cytomegalovirus *lacZ*-carrying plasmid as a control for transfection efficiency. At 24 h posttransfection, the cells were treated with IFN for 8 h and then subjected to a luciferase assay. Values for luciferase activity were normalized to those for β-galactosidase activity, and mean values of triplicate experiments are given.

Total RNAs were isolated from the cells by the use of TRIzol reagent (Invitrogen) and were then subjected to cDNA synthesis with a first-strand cDNA synthesis kit (SuperArray), followed by reverse transcription-PCR (RT-PCR) with a MultiGene-12 RT-PCR profiling kit (SuperArray) used according to the manufacturer's instructions. The RT-PCR products were analyzed by 1% agarose gel electrophoresis and were detected by ethidium bromide staining and/or autoradiography.

For Northern blot analyses, total RNAs were isolated from S11 tumor cells at 48 h posttransfection with M2-specific small inhibitory RNAs (siRNAs) or nonspecific scrambled siRNAs. A digoxigenin-labeled DNA probe specific for M2 was generated from pEF/M2-AU1 by use of a DNA high-prime random labeling kit (Roche), subjected to Northern blot analysis, and analyzed by chemiluminescence with a Fuji phosphorimager.

Cell extracts, immunoprecipitations, and immunoblots. For preparations of cell extracts for precipitation (6), transfected cells grown in 100-mm-diameter dishes were washed with ice-cold PBS and lysed with 1 ml of lysis buffer (150 mM NaCl, 1% Nonidet P-40, 50 mM Tris [pH 7.5], 0.2 mM EDTA) supplemented

with a protease inhibitor cocktail (Roche). The lysates were incubated on ice for 20 min prior to centrifugation for 30 min at 16,200 × *g* at 4°C. Supernatants with GST-M2 or M2 mutant fusion proteins were precipitated with glutathione-Sepharose beads for 2 h at 4°C. The precipitates were washed with lysis buffer five times, subjected to SDS-PAGE and immunoblotting with specific antibodies, and detected by chemiluminescence and a Fuji phosphorimager.

Reagents and antibodies. Mouse IFN-α, IFN-β, and IFN-γ were purchased from R&D Systems. STAT1, STAT2, STAT3, ISGF p48, JAK1, JAK2, Tyk2, tubulin, and p32 antibodies were purchased from Santa Cruz Biotechnology (Santa Cruz, Calif.). An anti-AU1 antibody was purchased from Bethyl Laboratories (Montgomery, Tex.).

RESULTS

Localization of M2 protein depends on cell type. To investigate the biological role of M2, we stably expressed the AU1-tagged M2 protein in mouse NIH 3T3 fibroblast cells and A20 B lymphocytes. As previously shown (29), the M2 protein migrated at an apparent molecular mass of 30 kDa for both cell types (Fig. 1A). Confocal microscopy was used to examine the intracellular localization of M2 in both cell types. Surprisingly, M2 showed different areas of localization (Fig. 1B). As previously shown (41), M2 was present in the cytoplasm and plasma membrane, with a low level of nuclear localization, in A20 B lymphocytes (Fig. 1B). In contrast, M2 was present primarily in the nucleus, with a detectable level of cytoplasmic and plasma membrane localization, in NIH 3T3 cells (Fig. 1B). These different localization patterns for M2 were also detected in other cell types: M2 was located in the cytoplasm and plasma membrane in mouse WEHI231 T/B hybrid lymphocytes and human BJAB B lymphocytes, whereas it showed predominantly nuclear localization in human 293T epithelial cells and EC5 endothelial cells (Fig. 1B). These results demonstrate that the M2 protein is present in the cytoplasm and plasma membrane, with a low level of nuclear localization, in lymphocytes, whereas it is present primarily in the nucleus, with a low level in the cytoplasm and plasma membrane, in fibroblast, epithelial, and endothelial cells.

The central proline and positively charged amino acids of M2 contribute to its nuclear localization. Despite its small coding sequence, M2 contains distinct regions, namely, four proline-rich regions and a central positively charged region. The multiple proline-rich regions are the N-terminal amino acids (aa) 3 to 15 (P_3 to P_{15}), the central aa 67 to 78 (P_{67} to P_{78}) and 95 to 115 (P_{95} to P_{115}), and the C-terminal aa 154 to 179 (P_{154} to P_{179}). The central positively charged region at aa 66 to 99 contains 12 arginine and lysine residues (RK region). This region also overlaps with one of the central proline-rich regions. To identify the potential nuclear localization signal in the M2 coding sequence, we generated deletion mutants of M2 as N-terminal fusions with GST. These GST-M2 mutants were M2 (1-150), M2 (1-100), M2 (50-100), M2 (100-192), M2 (1-50), and M2 (50-150) (Fig. 2A). GST fusion proteins were expressed in NIH 3T3 cells, and their localization was determined by immunostaining with an anti-GST antibody followed by confocal microscopy. The M2 (1-150) and M2 (50-150) mutants showed the similar intracellular localization pattern as GST-wt M2, being present primarily in the nucleus, with a low level of cytoplasmic and membrane localization (Fig. 2B). In contrast, the M2 (1-100), M2 (100-192), M2 (1-50), and M2 (50-100) mutants were localized primarily in the cytoplasm and plasma membrane, with much less nuclear localization (Fig. 2B). Finally, GST-M2 fusion protein showed essentially the same localization pattern as wt M2 in NIH 3T3 and A20 cells, indicating that the GST fusion did not affect M2 localization (Fig. 2B and data not shown). These results suggest that neither the N-terminal nor C-terminal proline-rich regions of M2 play a significant role in its nuclear localization, whereas the central region (aa 50 to 150) of M2 is not only required but is also sufficient for its nuclear localization (Fig. 2B).

The central region of M2 contains multiple proline residues and positively charged amino acids. To further investigate the roles of these amino acids in M2 nuclear localization, we introduced point mutations at the central proline residues or positively charged amino acids of M2. These mutants were M2 (P67-78/A), which contained alanine residues in place of proline residues 67, 70, 71, 73, and 78; M2 (P95-115/A), which contained alanine residues in place of proline residues 95, 98, 100, 102, 104, 106, 111, and 115; and M2 (RK/E), which contained glutamic acid residues in place of the positively charged arginine and lysine residues 66, 69, 74, 76, 79, 82, 83, 87, 88, 93, 97, and 99. GST-M2 fusion mutants were then expressed in NIH 3T3 cells, and their localization was determined by confocal microscopy. GST-M2 (P95-115/A) showed primarily nuclear localization, as was seen with GST-M2; GST-M2 (P67-78/A) exhibited both nuclear and cytoplasmic localization; and GST-M2 (RK/E) was present exclusively in the cytoplasm and the plasma membrane (Fig. 2). These results indicate that the central basic amino acids of M2 are essential for its nuclear localization, whereas the prolines (P67-78) within the central basic region also affect its nuclear localization.

Cellular p32 protein interacts with the central positively charged region of M2. To identify proteins that interacted with M2, we used the bacterially purified GST-M2 fusion protein in an affinity column for ^{35}S-labeled lysates of A20 B cells. A polypeptide with an apparent molecular mass of 32 kDa specifically interacted with the GST-M2 fusion protein, whereas it did not interact with the GST protein (Fig. 3A). To further characterize this cellular protein, we purified it from 10 liters of A20 B cells and analyzed it by mass spectrometry. The resulting protein was microsequenced and matched to known sequences. The 32-kDa band was identified as cellular acidic p32. p32 is a small acidic protein that has a broad range of distinct functions and associates with a wide array of cellular, viral, and bacterial proteins (7, 11, 25, 34, 40, 43, 44, 48, 65, 68, 73).

In vitro GST pull-down assays with lysates of A20 cells and immunoblotting with an anti-p32 antibody confirmed the interaction of M2 with p32 (data not shown). Additionally, the GST-M2 fusion was expressed in NIH 3T3 cells and then subjected to a mammalian GST pull-down assay followed by immunoblotting with an anti-p32 antibody. This also showed that GST-M2 interacted with the cellular p32 protein in NIH 3T3 cells (Fig. 3B). Furthermore, coimmunoprecipitation showed that the full-length M2 protein efficiently interacted with p32 in NIH 3T3 and A20 cells (Fig. 3C). To further delineate this interaction, we used GST-M2 mutants for GST pull-down assays with living cells. The GST-M2 (P67-78/A), GST-M2 (P95-115/A), GST-M2 (1-150), GST-M2 (1-100), GST-M2 (50-100), and GST-M2 (50-150) mutants interacted with the cellular p32 protein as efficiently as wt GST-M2 did, whereas GST-M2 (100-192) and GST-M2 (1-50) did not interact with the cellular p32 protein (Fig. 2A and 3D). Finally, the

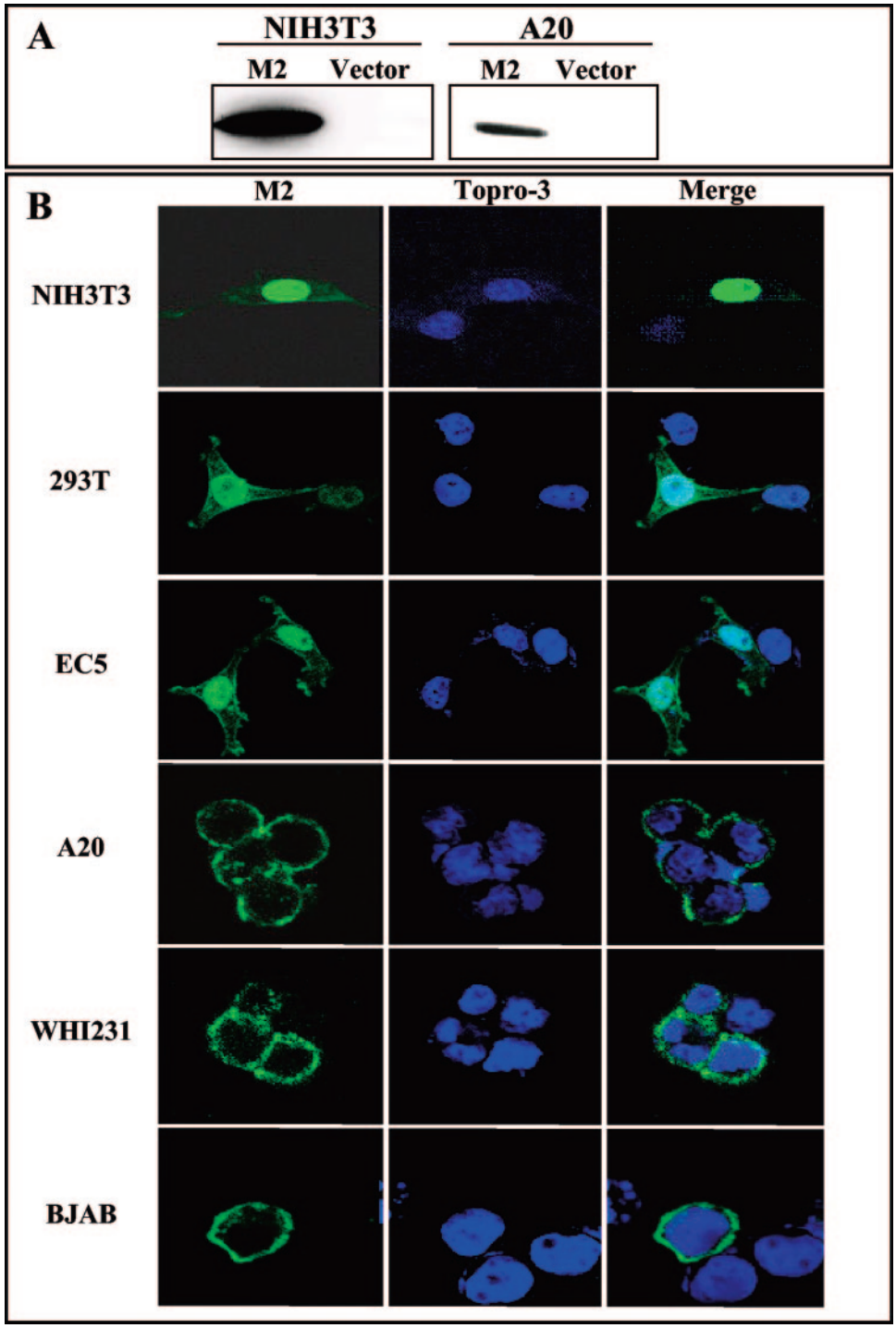

FIG. 1. γHV68 M2 expression and localization. (A) M2 expression. AU1-tagged M2 was stably expressed in NIH 3T3 and A20 cells. The M2 protein was detected by immunoprecipitation and immunoblotting with an anti-AU1 antibody. (B) Localization of M2. NIH 3T3 and A20 cells stably expressing AU1-tagged M2 were fixed, permeabilized, and incubated with an anti-AU1 antibody. Mouse WEHI231 T/B cells, human BJAB B cells, human epithelial cells, and human EC5 endothelial cells were transfected with the AU1-M2 expression vector. At 48 h posttransfection, the cells were fixed, permeabilized, and incubated with an anti-AU1 antibody. M2 localization in these cells was determined by confocal microscopy. Topro-3 was used for nuclear counterstaining.

GST-M2 (RK/E) mutant showed no detectable interaction with the cellular p32 protein (Fig. 2A and 3D). These results indicated that the central positively charged amino acids of M2 are necessary for the interaction with p32. This conclusion was further confirmed by the loss of the interaction of the full-length M2 (RK/E) mutant with the cellular p32 protein in NIH 3T3 cells (Fig. 3C). Thus, the basic amino acids within the M2 central region are essential for its interaction with p32.

A

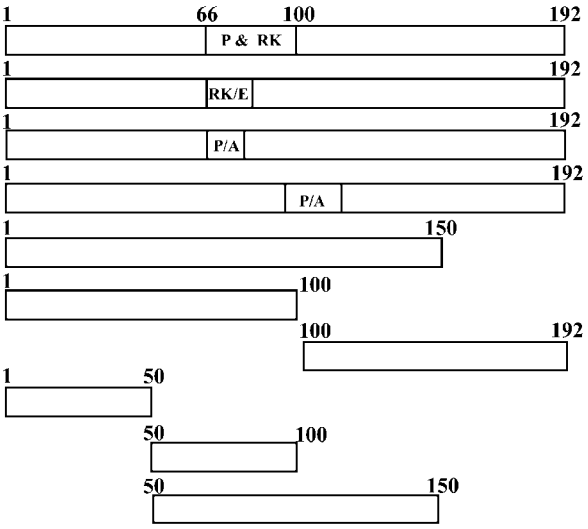

GST-M2	Localization	p32 binding
M2	Nucleus >> Cytoplasm	Yes
M2 (RK/E)	Cytoplasm	No
M2 (P67-78/A)	Nucleus > Cytoplasm	Yes
M2 (95-115/A)	Nucleus > Cytoplasm	Yes
M2 (1-150)	Nucleus >> Cytoplasm	Yes
M2 (1-100)	Nucleus & Cytoplasm	Yes
M2 (100-192)	Cytoplasm	No
M2 (1-50)	Cytoplasm	No
M2 (50-100)	Nucleus & Cytoplasm	Yes
M2 (50-150)	Nucleus > Cytoplasm	Yes

B

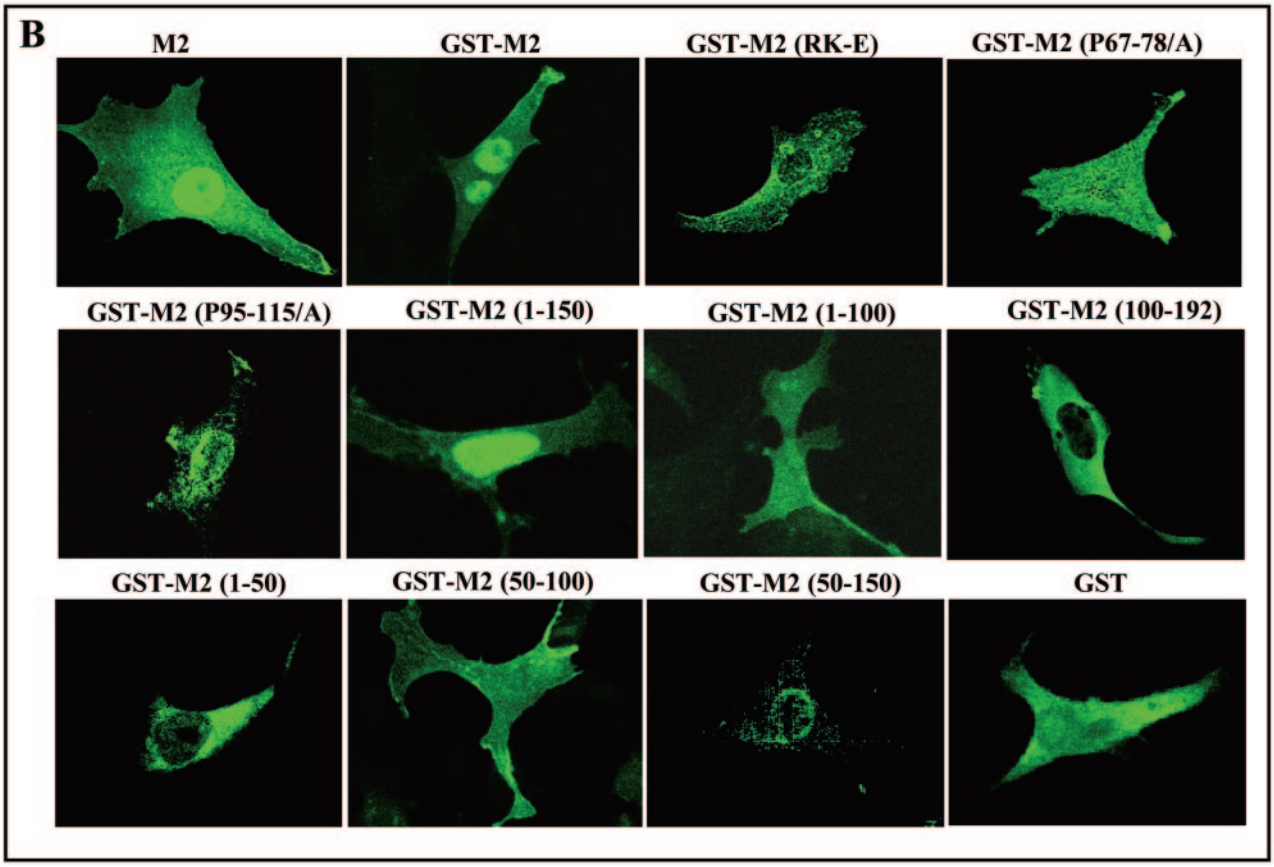

FIG. 2. Identification of M2 nuclear localization domain. (A) Summary of M2 mutations and their localization and p32 binding. The details for each M2 mutant are given in the text. All M2 mutants were cloned into the pEBG vector to yield GST fusion proteins for expression in mammalian cells. Nuclear ≫ cytoplasm, primarily nuclear localization; nuclear > cytoplasm, more localization in the nucleus than in the cytoplasm; nuclear and cytoplasm, even localization between the nucleus and the cytoplasm. (B) Characterization of M2 nuclear localization. NIH 3T3 cells transfected with M2, GST-wt M2, and GST-M2 mutants were fixed, permeabilized, incubated with an anti-GST antibody, and subjected to confocal microscopy.

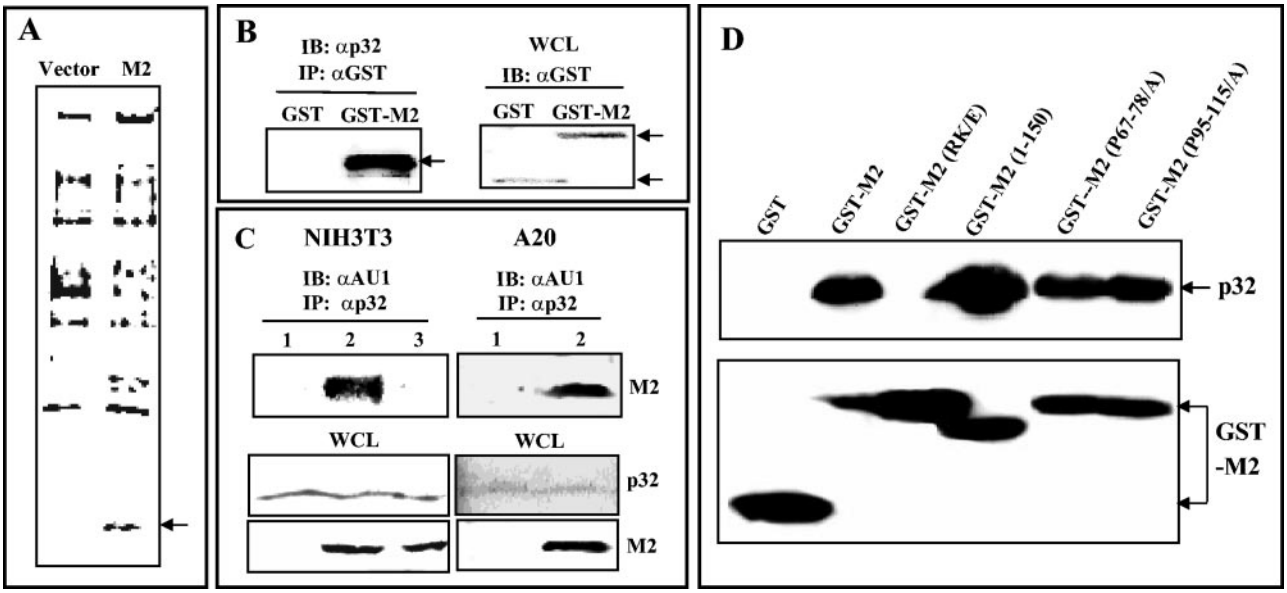

FIG. 3. M2 binding to cellular p32 protein. (A) Purification of M2-binding cellular proteins. The GST-M2 fusion protein purified from *Escherichia coli* was mixed with [^{35}S]methionine- and [^{35}S]cysteine-labeled extracts of A20 B cells. The precipitated complexes were separated through 4 to 12% Tris-Bis gels and autoradiographed by use of a phosphorimager. The arrow indicates the p32 protein. (B) GST-M2 interaction with p32 in NIH 3T3 cells. NIH 3T3 cells were transiently transfected with a GST or GST-M2 expression vector. At 48 h posttransfection, cell lysates were used for GST pull-down assays with a glutathione-Sepharose column (IP). Purified proteins were separated by SDS-PAGE and analyzed by immunoblotting (IB) with an anti-p32 antibody. Whole-cell lysates (WCL) were used to detect GST and GST-M2 proteins (arrows). (C) Interaction of full-length M2, but not the M2 (RK/E) mutant, with cellular p32. NIH 3T3 cells stably expressing vector alone (lane 1), wt M2 (lane 2), or the M2 (RK/E) mutant (lane 3) and A20 cells stably expressing vector (lane 1) or wt M2 (lane 2) were used for immunoprecipitation with an anti-p32 antibody, followed by immunoblotting with an anti-AU1 antibody. Whole-cell lysates were used to detect endogenous p32, wt M2, and the M2 (RK/E) mutant. (D) Mapping of p32 interacting region in M2. At 48 h posttransfection with GST, GST-M2, or GST-M2 mutants, NIH 3T3 cells were used for GST pull-down assays, followed by immunoblotting with an anti-p32 antibody. Whole-cell lysates were used to detect GST and GST-M2 fusion proteins. Arrows indicate p32, GST, and GST-M2 proteins.

M2 colocalizes with p32. The cellular p32 protein has been found in each of the main cellular compartments, including mitochondria, the nucleus, and the cytoplasm; it is also thought to be located at the plasma membrane and to be secreted into the extracellular matrix (7, 43, 63). Particularly, the EBV EBNA1, HVS ORF73, and HSV ICP27 (IE63) proteins have been shown to interact with p32 and to translocate p32 from the cytoplasm to the nucleus (7, 11, 25, 68). We found that the p32 protein was principally located in the cytoplasmic regions of A20 and NIH 3T3 cells (Fig. 4). Since the M2 protein had a cell-type-dependent localization and efficiently interacted with p32, we tested whether M2 colocalized with p32 in A20 and NIH 3T3 cells and whether M2 ultimately recruited p32 into the nucleus in NIH 3T3 cells. A20 and NIH 3T3 cells expressing AU1-tagged M2 were fixed, permeabilized, and incubated with anti-AU1 and anti-p32 antibodies. When M2 was expressed in A20 B cells, M2 and p32 showed extensive colocalization primarily in the cytoplasm (Fig. 4). However, when M2 was expressed in NIH 3T3 cells, M2 was not only located primarily in the nucleus, but also efficiently recruited p32 into the nucleus, resulting in the extensive colocalization of M2 and p32 in the nucleus (Fig. 4). In striking contrast, when the M2 (RK/E) mutant was expressed in NIH 3T3 cells, both M2 (RK/E) and p32 were present in the cytoplasmic region, with little colocalization (Fig. 4). These results indicate that M2 extensively colocalizes with p32 in both A20 and NIH 3T3 cells and that the M2 interaction subsequently recruits p32 into the nucleus in NIH 3T3 cells.

M2 antagonizes IFN-α/β- and IFN-γ-mediated transcriptional activation. Previous studies have shown that IFN-α/β is essential for the control of acute γHV68 infections, while IFN-γ has a vital role in regulating chronic γHV68 infections (69). Furthermore, M2 is a latency-associated gene and is differentially required for viral latency and reactivation, indicating its potential role in the establishment and maintenance of a γHV68 latent infection in the face of an active host immune response, such as IFN control. Based on these facts, we hypothesized that M2 might play a role in controlling IFN-mediated antiviral signaling. To test the potential role of M2 as an IFN antagonist, we measured the transcriptional activities of IFN-regulated promoters by using a luciferase reporter gene. Since IFN-α/β and IFN-γ act on overlapping but distinct sets of *cis*-acting elements (36), we employed two luciferase constructs that contained the different *cis*-acting elements, i.e., the IFN-stimulated response element (ISRE) of the IFN-stimulated gene ISG15 (ISG15-ISRE) and the IFN-γ activation site (GAS). A20 and NIH 3T3 cells expressing the vector only or M2 were transfected with a luciferase reporter plasmid and a control β-galactosidase plasmid, pGK-β-Gal. At 24 h posttransfection, the cells were incubated for 8 h in the presence or absence of IFN-α, IFN-β, or IFN-γ. Luciferase activities were normalized for transfection efficiency by use of the β-galactosidase activity. ISG15-ISRE activity was induced approximately 10-fold in vector-expressing A20 cells upon IFN-α stimulation, whereas it was not induced or was minimally induced in M2-expressing A20 cells under the same conditions (Fig.

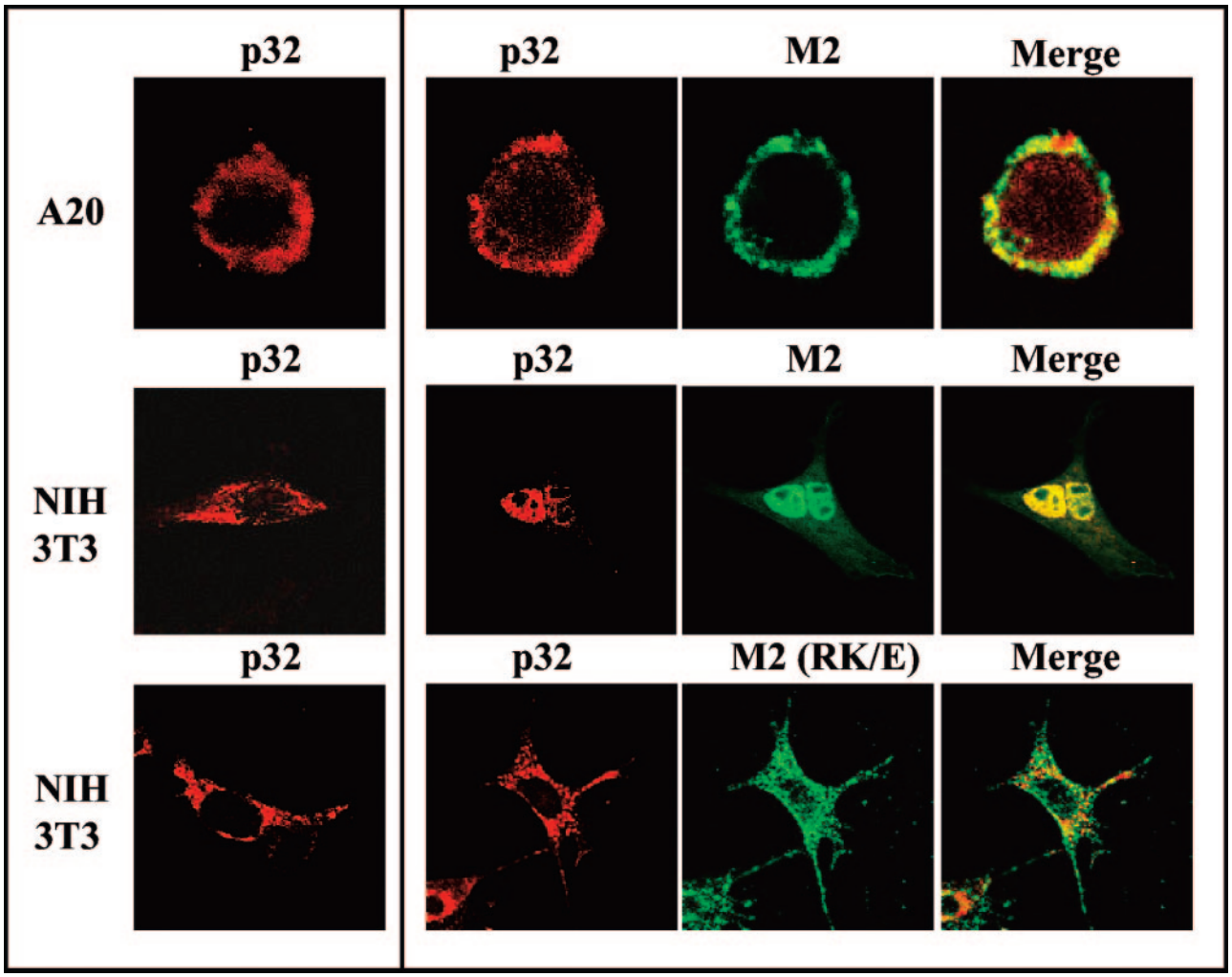

FIG. 4. M2 and p32 localization in A20 and NIH 3T3 cells. (Left panel) The cytoplasmic localization of p32 was detected in A20 and NIH 3T3 cells. (Right panel) M2 and p32 were detected in A20-M2, NIH 3T3-M2, and NIH 3T3-M2 (RK/E) cells. The cells were costained with anti-AU1 (green) and anti-p32 (red) antibodies. Yellow areas in the merged panels indicate colocalization of the red and green labels.

5A). The level of IFN-β-activated ISG15-ISRE activity in M2-expressing NIH 3T3 cells was also repressed approximately 10-fold in the absence of IFN compared to that in vector-expressing NIH 3T3 cells (Fig. 5B). Furthermore, IFN-β treatment had almost no effect on ISG15-ISRE activity in M2-expressing NIH 3T3 cells, whereas it induced detectable ISG15-ISRE activity in vector-expressing NIH 3T3 cells (Fig. 5B). Similarly, GAS activity was also strongly induced in vector-expressing A20 cells upon IFN-γ stimulation, whereas its level of activation was drastically repressed in M2-expressing A20 cells under the same conditions (Fig. 5A). Finally, M2 expression also showed a strong inhibition of IFN-γ-activated GAS activities in NIH 3T3 cells (Fig. 5B). No luciferase was detected in either cell type transfected with the GAS_{mutant} element, which lacks binding to the STAT1 transcriptional factor (38; also data not shown). In striking contrast, the M2 (RK/E) mutant was incapable of inhibiting IFN-mediated transcriptional activation in either A20 or NIH 3T3 cells, suggesting that the M2 interaction with p32 may play a role in its inhibition of IFN-mediated transcriptional activation (Fig. 5). Furthermore, RT-PCR analysis showed that the induction level of IFN-induced protein with tetratricopeptide repeats 1 (IfiT1) was lower in M2-expressing cells upon IFN-α stimulation than in control cells (Fig. 5C). These results demonstrate that M2 expression in both A20 and NIH 3T3 cells leads to a marked repression of IFN-α/β- and IFN-γ-mediated transcriptional activation.

M2 downregulates STAT 1 and/or STAT2 expression. While STAT proteins are normally long-lived, herpesvirus infections often result in the effective loss of IFN-responsive STAT expression. To elucidate the potential M2-mediated inhibitory mechanism of IFN signal transduction, we compared the expression levels of JAK/STAT signaling components in M2-expressing cells with those in control cells. Equivalent amounts of protein extracts from A20-vector, A20-M2, NIH 3T3-vector, and NIH 3T3-M2 cells were used for immunoblot assays with various antibodies that react with JAK/STAT pathway components. A20 and NIH 3T3 cells expressing the M2 (RK/E) mutant were also included in these assays. The amounts of STAT2 protein were considerably reduced in both NIH

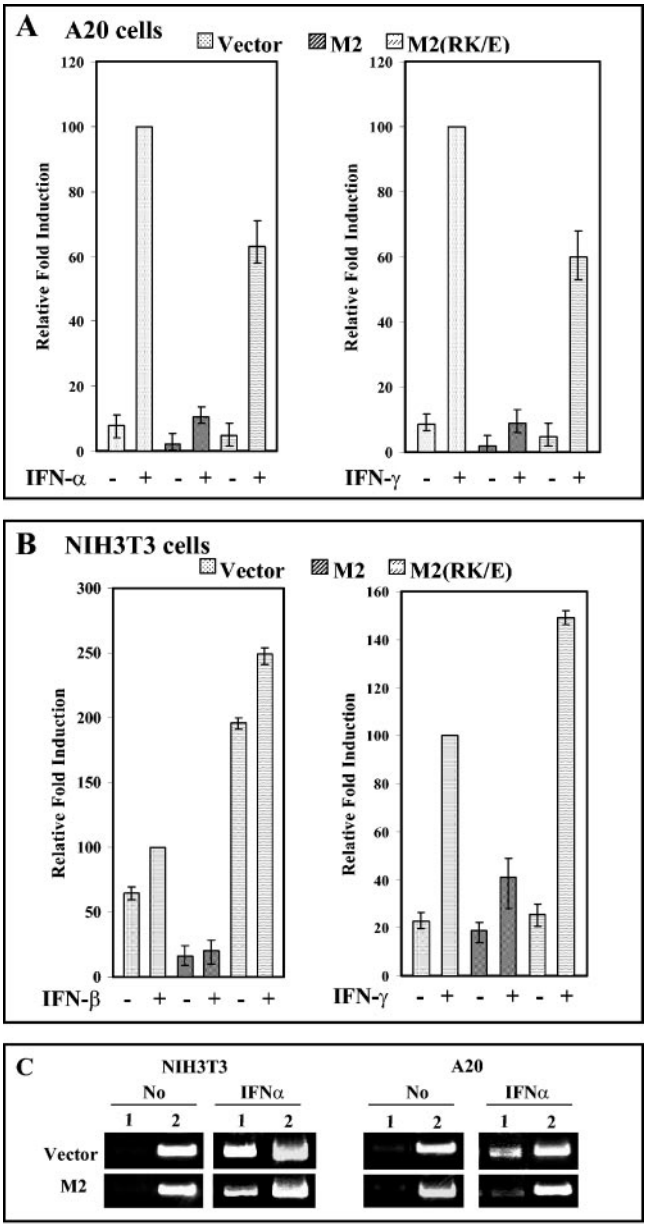

FIG. 5. Inhibition of IFN-β and IFN-γ signaling by M2 expression. A20 cells (A) and NIH 3T3 cells (B) expressing either M2 or the M2 (RK/E) mutant were transfected with an IFN-α/β-responsive ISRE-luciferase reporter gene or a IFN-γ-responsive GAS-luciferase reporter gene together with pGK-β-Gal. Transfected cells were then treated with 1,000 U of IFN-α/β per ml or with 5 ng of IFN-γ per ml for 8 h prior to lysis and luciferase assays. Luciferase values were normalized to β-galactosidase activities. Relative induction is expressed compared with the luciferase activity of IFN-treated A20-vector and NIH 3T3-vector cells, which was set at 100-fold. The results represent average values from three individual experiments, and the error bars indicate standard deviations. (C) Analysis of interferon-induced cellular gene expression. Total RNAs were isolated from NIH 3T3-vector, NIH 3T3-M2, A20-vector, and A20-M2 cells with or without IFN-α treatment (1,000 U per ml) and were subjected to RT-PCR analysis for IfiT1 expression (lanes 1). GAPDH expression (lanes 2) was included as a control. Amplified DNA fragments were separated in a 1% agarose gel and then photographed.

3T3-M2 and A20-M2 cells compared to those in NIH 3T3-vector and A20-vector cells, whereas a reduction in STAT1 was detected only for NIH 3T3-M2 cells, not A20-M2 cells (Fig. 6A and B). No detectable alteration in the amount of JAK1/2 kinases, TYK2 kinase, or ISGF p48 was observed for either A20-M2 or NIH 3T3-M2 cells (Fig. 6A and B). Furthermore, the expression of the M2 (RK/E) mutant, which was not able to inhibit IFN-mediated transcriptional activation, showed no effect on STAT1 and/or STAT2 protein expression in either A20 or NIH 3T3 cells (Fig. 6A and B).

To correlate M2 expression with the reduction in the amount of STAT2 protein, we transfected an M2-specific siRNA or a nonspecific scrambled siRNA into latently γHV68-infected S11 B lymphoma cells. At 48 h posttransfection with the siRNA, total RNAs were used to show the depletion of M2 mRNA in siRNA-treated S11 cells (Fig. 6C). Cellular extracts were also used for an immunoblot analysis to examine STAT2 expression. This analysis showed that the suppression of M2 expression in S11 cells resulted in the restoration of STAT2 expression (Fig. 6C). This effect was specific because the suppression of M2 expression by the siRNA did not affect tubulin expression under the same conditions (Fig. 6C). This result shows the inverse correlation between M2 expression and STAT2 expression in virus-infected B lymphoma cells.

To further define the molecular mechanism of STAT downregulation induced by the γHV68 M2 protein, we compared the transcriptional profiles of mouse JAK and STAT family genes between vector-expressing control cells and M2-expressing target cells. While the transcription profiles of most JAK/STAT family genes were not affected by M2 expression, the levels of STAT2 and STAT6 mRNAs were reduced in NIH 3T3-M2 and A20-M2 cells compared to those in NIH 3T3-vector and A20-vector cells (Fig. 6D). In contrast, M2 (RK/E) mutant expression showed no downregulation of the STAT2 and STAT6 mRNA levels (Fig. 6D). Interestingly, the level of STAT1 mRNA was not altered by M2 expression in both cell types, suggesting that the M2-mediated downregulation of STAT1 expression occurs at the posttranscriptional level (Fig. 6D). This notion was further supported by a treatment with the proteasome inhibitor MG132 that substantially enhanced the amount of STAT1 protein, but not STAT2 protein, in M2-expressing cells (Fig. 6E). These results collectively showed that M2 expression downregulates STAT1 expression at the posttranscriptional level, whereas it downregulates STAT2/6 expression at the transcriptional level.

DISCUSSION

Upon viral infection, the major counterassault mounted by the host immune system is the activation of the IFN-mediated antiviral pathway as a mechanism to restrict viral replication. In this report, we demonstrated that the latency-associated M2 gene of γHV68 functions as a repressor to inhibit IFN-mediated transcriptional activation. Interestingly, the M2 protein displayed a cell-type-dependent localization: it was primarily localized in the cytoplasm and plasma membrane in lymphocytes and in the nucleus in fibroblast and epithelial cells. Furthermore, we showed that M2 interacted with the cellular p32 acidic protein through its central basic region and that this interaction possibly correlates with its ability to inhibit IFN-

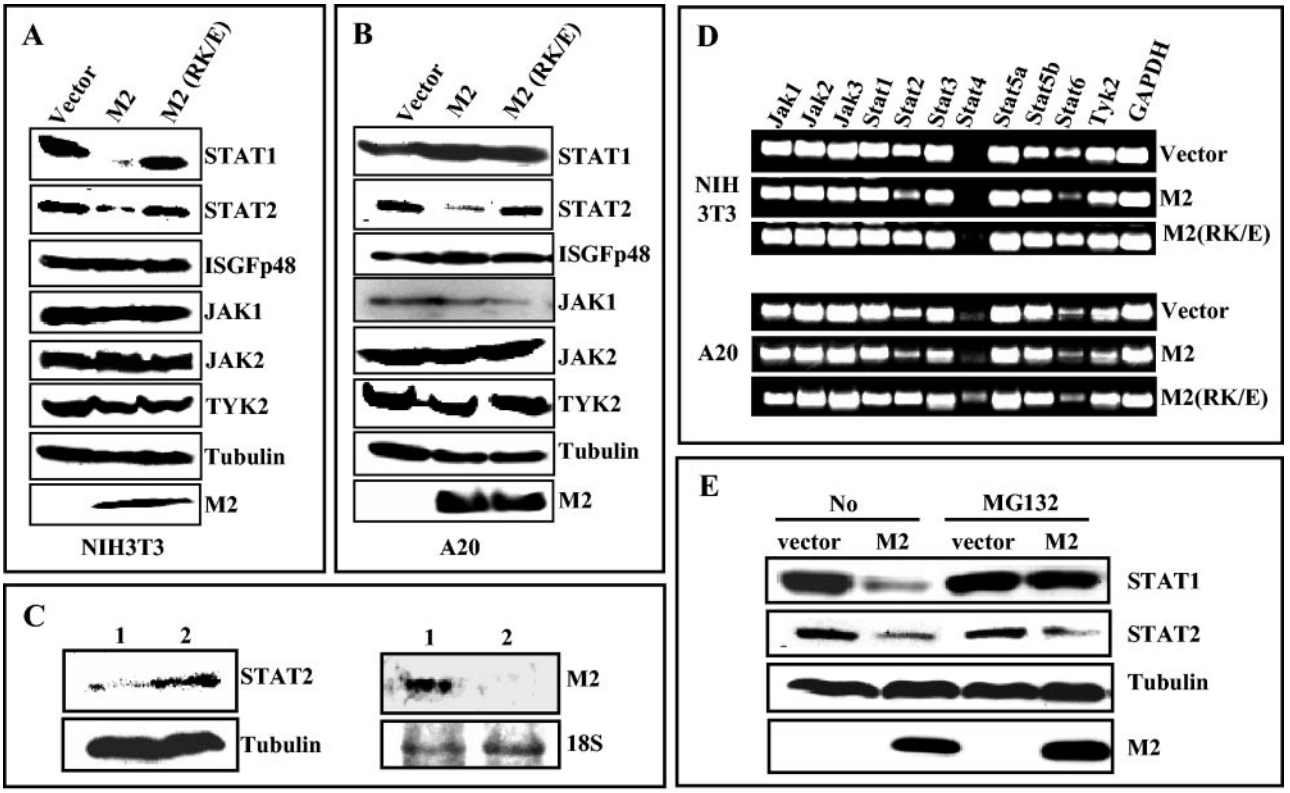

FIG. 6. Downregulation of STAT expression by M2. (A and B) Immunoblot analysis of JAK/STAT family proteins. Approximately 20 μg of cell extracts of A20-vector, A20-M2, A20-M2 (RK/E), NIH 3T3-vector, NIH 3T3-M2, and NIH 3T3-M2 (RK/E) cells were separated by SDS-PAGE and analyzed by immunoblotting with antibodies against STAT1, STAT2, ISGF p48, JAK1, JAK2, Tyk2, tubulin, and AU1-tagged M2. (C) Suppression of M2 expression by siRNA treatment. S11 cells were transfected with nonspecific scrambled siRNAs (lanes 1) or M2-specific siRNAs (lanes 2). At 48 h posttransfection, whole-cell lysates and total RNAs were used for immunoblot analysis with anti-STAT2 and anti-tubulin antibodies (left) and for Northern blot analysis with an M2-specific probe (right), respectively. 18S was included as a loading control in Northern blots (bottom of right panel). (D) RT-PCR analysis of JAK/STAT family gene expression. Total RNAs isolated from A20-vector, A20-M2, A20-M2 (RK/E), NIH 3T3-vector, NIH 3T3-M2, and NIH 3T3-M2 (RK/E) cells were subjected to quantitative RT-PCRs with a mouse JAK-STAT Multi-Gene profiling kit. Amplified DNA fragments were separated in a 1% agarose gel and then photographed. (E) STAT expression upon MG132 treatment. After 6 h of treatment with or without the proteasomal inhibitor MG132, whole-cell lysates were prepared from NIH 3T3-vector and NIH 3T3-M2 cells, separated by SDS-PAGE, and subjected to immunoblotting with anti-STAT1, anti-STAT2, anti-tubulin, and anti-AU1 antibodies.

mediated transcriptional activation. Finally, the downregulation of STAT expression was the likely mechanism underlying the M2-mediated inhibition of IFN signaling. These results demonstrate for the first time that γHV68 may harbor a latency-associated M2 gene to antagonize IFN-mediated host innate immunity and may play an important role in the establishment and maintenance of viral latency in infected animals.

Several reports have shown that γHV68 M2 is a latency-associated gene and that its transcripts are detected in latently infected splenocytes and peritoneal exudate cells as well as in a latently γHV68-infected B-lymphoma cell line (29). While mutation of the M2 gene did not affect the ability of the virus to replicate in tissue culture, mutant virus acute-phase replication in the spleen has been shown to be lower than that of wild-type and marker rescue viruses after intraperitoneal inoculation (30). Upon intranasal inoculation, however, M2 mutant viruses exhibited a significantly lower level of latency establishment and reactivation frequency in the spleen (30, 41). Despite these detailed studies, however, the biochemical function of M2 has not been assessed. The human gammaherpesviruses EBV and KSHV have both been shown to efficiently block the antiviral IFN response through distinct mechanisms (38, 39, 45). We also found that γHV68 harbors the latency-associated M2 protein to inhibit IFN-mediated transcriptional activation. However, the modes of action of these viruses for the inhibition of IFN-mediated transcriptional activation are likely different from each other: EBV BZLF1 downregulates IFN-γ receptor gene expression (45), KSHV vIRF1 interacts with and inhibits the p300 transcriptional coactivator (37, 39), and γHV68 M2 downregulates STAT expression. Furthermore, M2 showed divergent phenotypes in B lymphocytes and fibroblast cells due to its differential localization patterns: M2 downregulated STAT1 and STAT2 expression in fibroblast cells, whereas it downregulated only STAT2 expression in B lymphocytes. The STAT2 mRNA level was downregulated to a detectable degree in both M2-expressing A20 and NIH 3T3 cells, suggesting that STAT2 expression is likely regulated by M2 at the transcriptional level. In contrast, the M2 (RK/E) mutant, which eliminated p32 binding activity, neither suppressed the STAT2 mRNA level nor downregulated the STAT2 protein level, indicating that the interaction with the p32 protein may play a role in the downregulation of STAT2

expression. Moreover, STAT2 expression in latently γHV68-infected S11 cells was restored by the siRNA-mediated suppression of M2 expression, indicating that M2 is responsible for the downregulation of STAT2 expression in virus-infected cells. Further studies will be directed toward investigating the detailed mechanism of M2-mediated STAT downregulation.

The downregulation of STAT1 expression induced by M2 is likely more complex than that of STAT2 because it was detected only in NIH 3T3 fibroblast cells, not in A20 B cells. Furthermore, the STAT1 mRNA level was not altered by M2 expression in either cell type. However, we observed that treatment with the proteasome inhibitor MG132 was able to recover STAT1 protein expression in M2-expressing NIH 3T3 cells, suggesting that M2 may facilitate the proteasome-dependent degradation of the STAT1 protein. While STAT proteins are normally stable and long-lived, paramyxovirus infections often result in an efficient loss of IFN-responsive STAT1 and STAT2. The expression of SV5 and the hPIV2-encoded V protein has been shown to be sufficient to mediate the destruction of the STAT1 and STAT2 proteins (14, 47). Recently, SV5 and hPIV2 V expression was shown to induce the polyubiquitination and degradation of STAT1 and STAT2 by interacting with a complex containing damaged DNA binding protein 1 and cullin 4A ubiquitin ligase (61). HSV has been also shown to interfere with the IFN signaling pathway at multiple steps, including the downregulation of JAK1 and STAT2, the inhibition of STAT1 tyrosine phosphorylation, and disruption of the nuclear structure (9, 10, 26, 27). Furthermore, HSV-1 ICP0, a promiscuous transactivator, has been shown to act as a unimolecular E3 ubiquitin ligase and to promote ubiquitin-protein ligation, which is likely to be critical for the inhibition of the host IFN response (10, 64). While γHV68 M2 does not share any detectable homology with SV5, the hPIV2 V protein, and the HSV-1 ICP0 protein, it may target the cellular proteasomal complex to achieve diverse effects on cellular physiology. This hypothesis is under active investigation.

STAT6 is primarily associated with signaling by two cytokines with a biological overlap, i.e., interleukin-4 (IL-4) and IL-13, and STAT6 activity plays an important role in the development of cells with a Th2 cytokine phenotype (58). In addition, IFN-α stimulation has also been shown to activate complexes containing STAT6; these complexes are predominantly detected in B cells (24). Furthermore, the activation of STAT6 by IFN-α in B cells is accompanied by the formation of novel STAT2-STAT6 complexes, which may allow for the modulation of target genes in a cell type-specific manner (24). M2 expression also reduced the level of STAT6 mRNA in both NIH 3T3 fibroblasts and A20 B cells. This suggests that the downregulation of STAT6 expression induced by M2 not only may affect IFN-mediated antiviral activity, but also may influence the Th2 cytokine-mediated host immune response. Both activities may ultimately contribute to the establishment and maintenance of viral latency.

The EBV EBNA-1, HSV-1 IE63, and HVS ORF73 proteins have been shown to interact with the cellular p32 protein (7, 11, 25, 68). These interactions trigger the accumulation of p32 in the nucleus. In addition, the binding of HVS ORF73 to p32 is mediated by an amino-terminal arginine-rich domain that contains two functionally distinct nuclear localization signals (25). Furthermore, two N-terminal regions of EBV EBNA-1 that interact with p32 also contain arginine-rich repeats. We showed that M2 interacted with p32 through the central arginine- and lysine-rich basic region and that this interaction induced the translocation of p32 to the nucleus. Despite the equivalent levels of interaction of M2 with p32 in both NIH 3T3 and A20 cells, the nuclear localization of M2 and p32 was detected predominantly in NIH 3T3 cells, not A20 cells. This differential localization pattern of the M2 and p32 complex may ultimately cause different effects on STAT protein expression. Interestingly, the cellular p32 protein has been shown to occasionally undergo multiple posttranslational processing steps, resulting in three different forms: the full-length form (aa 1 to 282), a partially mature form (aa 33 to 282), and a fully mature form (aa 81 to 282) (68). More interestingly, the full-length form of p32 remains in the cytoplasm, the partially mature form displays diffused localization over both the cytoplasm and the nucleus, and the fully mature form is present predominantly in the nucleus (68). This suggests that M2 may interact with the different forms of p32 protein in different cell types, which ultimately dictates their localization. On the other hand, additional cellular proteins that are present only in adherent cells but not in cells in suspension may be involved in the interaction of M2 with p32 and thereby in their nuclear localization in adherent cells. Furthermore, our mutational analysis indicated that the central basic amino acids of M2 are required for its nuclear localization. It is also possible that differential modifications, such as phosphorylation and ubiquitination, of this basic region of M2 in fibroblast and epithelial cells may direct its nuclear localization or that other cellular factors are recruited to shuttle M2 between the nucleus and the cytoplasm. The detailed molecular mechanism of the nuclear localization of M2 needs to be further characterized. Furthermore, the connection of M2 localization, the M2 interaction with p32, and M2 inhibition of the IFN signaling pathway still needs to be investigated in more detail.

In summary, we demonstrated that γHV68 latency-associated M2 inactivates IFN-mediated host innate immunity by targeting STAT expression. This effect may create a favorable milieu for the establishment and/or maintenance of viral latency. Although the full significance of M2-mediated effects on IFN signal transduction needs to be studied further, our study provides a possible insight into the latency mechanism of γHV68. Future studies of the molecular mechanisms of γHV68 M2-mediated inhibition of IFN signal transduction may lead to a better understanding of viral latency and also may provide a novel means for investigating cellular IFN regulatory systems.

ACKNOWLEDGMENTS

We thank D. Hayward and A. Whitehouse for p32 constructs, S. Speck and S. Virgin for γHV68, J. Stewart and J. Sample for S11 cells, S. Gygi for mass spectrometry analysis, K. Boisvert for confocal microscopy, J. Macke for manuscript editing, and members of our laboratory for helpful discussions and comments.

This work was partly supported by U.S. Public Health Service grants CA31363, CA82057, AI38131, and RR00168. J. Jung is a Leukemia and Lymphoma Scholar.

REFERENCES

1. **Bach, E. A., M. Aguet, and R. D. Schreiber.** 1997. The IFNγ receptor: a paradigm for cytokine receptor signaling. Annu. Rev. Immunol. **15:**563–591.
2. **Billiau, A.** 1996. Interferon-γ: biology and role in pathogenesis. Adv. Immunol. **62:**61–130.

3. **Blasdell, K., C. McCracken, A. Morris, A. A. Nash, M. Begon, M. Bennett, and J. P. Stewart.** 2003. The wood mouse is a natural host for *Murine herpesvirus 4.* J. Gen. Virol. **84:**111–113.
4. **Blaskovic, D., D. Stanekova, and J. Rajcani.** 1984. Experimental pathogenesis of murine herpesvirus in newborn mice. Acta Virol. **28:**225–231.
5. **Blaskovic, D., M. Stancekova, J. Svobodova, and J. Mistrikova.** 1980. Isolation of five strains of herpesviruses from two species of free living small rodents. Acta Virol. **24:**468.
6. **Bontron, S., N. Lin-Marq, and M. Strubin.** 2002. Hepatitis B virus X protein associated with UV-DDB1 induces cell death in the nucleus and is functionally antagonized by UV-DDB2. J. Biol. Chem. **277:**38847–38854.
7. **Bryant, H. E., D. A. Matthews, S. Wadd, J. E. Scott, J. Kean, S. Graham, W. C. Russell, and J. B. Clements.** 2000. Interaction between herpes simplex virus type 1 IE63 protein and cellular protein p32. J. Virol. **74:**11322–11328.
8. **Cassady, K. A., M. Gross, G. Y. Gillespie, and B. Roizman.** 2002. Second-site mutation outside of the U_S10–12 domain of $\Delta\gamma_1$34.5 herpes simplex virus 1 recombinant blocks the shutoff of protein synthesis induced by activated protein kinase R and partially restores neurovirulence. J. Virol. **76:**942–949.
9. **Chee, A. V., and B. Roizman.** 2004. Herpes simplex virus 1 gene products occlude the interferon signaling pathway at multiple sites. J. Virol. **78:**4185–4196.
10. **Chelbi-Alix, M. K., and H. de The.** 1999. Herpes virus induced proteasome-dependent degradation of the nuclear bodies-associated PML and Sp100 proteins. Oncogene **18:**935–941.
11. **Chen, M. R., J. F. Yang, C. W. Wu, J. M. Middeldorp, and J. Y. Chen.** 1998. Physical association between the EBV protein EBNA-1 and p32/TAP/hyaluronectin. J. Biomed. Sci. **5:**173–179.
12. **Darnell, J. E., Jr.** 1997. STATs and gene regulation. Science **277:**1630–1635.
13. **Deck, T., D. J. Lew, J. Mirkovitch, and J. E. Darnell, Jr.** 1991. Cytoplasmic activation of GAF, an IFN-gamma-regulated DNA-binding factor. EMBO J. **10:**927–932.
14. **Didcock, L., D. F. Young, S. Goodbourn, and R. E. Randall.** 1999. The V protein of simian virus 5 inhibits interferon signaling by targeting STAT1 for proteasome-mediated degradation. J. Virol. **73:**9928–9933.
15. **Efstathiou, S., Y. M. Ho, S. Hall, C. J. Styles, S. D. Scott, and U. A. Gompels.** 1990. Murine herpesvirus 68 is genetically related to the gammaherpesviruses Epstein-Barr virus and herpesvirus saimiri. J. Gen. Virol. **71:**1365–1372.
16. **Flano, E., S. M. Husain, J. T. Sample, D. L. Woodland, and M. A. Blackman.** 2000. Latent murine gamma-herpesvirus infection is established in activated B cells, dendritic cells, and macrophages. J. Immunol. **165:**1074–1081.
17. **Fu, X. Y., C. Schindler, T. Improta, R. Aebersold, and J. E. Darnell, Jr.** 1992. The proteins of ISGF-3, the interferon alpha-induced transcriptional activator, define a gene family involved in signal transduction. Proc. Natl. Acad. Sci. USA **89:**7840–7843.
18. **Gao, J., B. P. Be, Y. Han, S. Choudhary, R. Ransohoff, and A. K. Banerjee.** 2001. Human parainfluenza virus type 3 inhibits gamma interferon-induced major histocompatibility complex class II expression directly and by inducing alpha/beta interferon. J. Virol. **75:**1124–1131.
19. **Garcia-Sastre, A.** 2001. Inhibition of interferon-mediated antiviral responses by influenza A viruses and other negative-strand RNA viruses. Virology **279:**375–384.
20. **Garcin, D., P. Latorre, and D. Kolakofsky.** 1999. Sendai virus C proteins counteract the interferon-mediated induction of an antiviral state. J. Virol. **73:**6559–6565.
21. **Goodbourn, S., L. Didcock, and R. E. Randall.** 2000. Interferons: cell signaling, immune modulation, antivirus response and virus countermeasures. J. Gen. Virol. **81:**2341–2364.
22. **Gotoh, B., K. Takeuchi, T. Komatsu, and J. Yokoo.** 2003. The STAT2 activation process is a crucial target of Sendai virus C protein for the blockade of alpha interferon signaling. J. Virol. **77:**3360–3370.
23. **Gotoh, B., T. Komatsu, K. Takeuchi, and J. Yokoo.** 2002. Paramyxovirus strategies for evading the interferon response. Rev. Med. Virol. **12:**337–357.
24. **Gupta, S., M. Jiang, and A. B. Pernis.** 1999. IFN-alpha activates Stat6 and leads to the formation of Stat2:Stat6 complexes in B cells. J. Immunol. **163:**3834–3841.
25. **Hall, K. T., M. S. Giles, M. A. Calderwood, D. J. Goodwin, D. A. Matthews, and A. Whitehouse.** 2002. The Herpesvirus saimiri open reading frame 73 gene product interacts with the cellular protein p32. J. Virol. **76:**11612–11622.
26. **Harle, P., B. Sainz, Jr., D. J. Carr, and W. P. Halford.** 2002. The immediate-early protein, ICP0, is essential for the resistance of herpes simplex virus to interferon-alpha/beta. Virology **293:**295–304.
27. **He, B., M. Gross, and B. Roizman.** 1997. The γ134.5 protein of herpes simplex virus 1 complexes with protein phosphatase 1α to dephosphorylate the α subunit of the eukaryotic translation initiation factor 2 and preclude the shutoff of protein synthesis by double-stranded RNA-activated protein kinase. Proc. Natl. Acad. Sci. USA **94:**843–848.
28. **Honore, B., P. Madsen, H. H. Rasmussen, J. Vandekerckhove, J. E. Celis, and H. Leffers.** 1993. Cloning and expression of a cDNA covering the complete coding region of the P32 subunit of human pre-mRNA splicing factor SF2. Gene **134:**283–287.
29. **Husain, S. M., E. J. Usherwood, H. Dyson, C. Coleclough, M. A. Coppola, D. L. Woodland, M. A. Blackman, J. P. Stewart, and J. T. Sample.** 1999. Murine gammaherpesvirus M2 gene is latency-associated and its protein a target for $CD8^+$ T lymphocytes. Proc. Natl. Acad. Sci. USA **96:**7508–7513.
30. **Jacoby, M. A., H. W. Virgin IV, and S. H. Speck.** 2002. Disruption of the M2 gene of murine gammaherpesvirus 68 alters splenic latency following intranasal, but not intraperitoneal, inoculation. J. Virol. **76:**1790–1801.
31. **Kerr, I. M., A. P. Costa-Pereira, B. F. Lillemeier, and B. Strobl.** 2003. Of JAK, STATs, blind watchmakers, jeeps and trains. FEBS Lett. **546:**1–5.
32. **Khan, S., A. Zimmermann, M. Basler, M. Groettrup, and H. Hengel.** 2004. A cytomegalovirus inhibitor of gamma interferon signaling controls immunoproteasome induction. J. Virol. **78:**1831–1842.
33. **Kotenko, S. V., and S. Pestka.** 2000. Jak-Stat signal transduction pathway through the eyes of cytokine class II receptor complexes. Oncogene **19:**2557–2565.
34. **Krainer, A. R., A. Mayeda, D. Kozak, and G. Binns.** 1991. Functional expression of cloned human splicing factor SF2: homology to RNA-binding proteins, U1 70K and *Drosophila* splicing regulators. Cell **66:**383–394.
35. **Kubota, T., N. Yokosawa, S. Yokota, and N. Fujii.** 2001. C terminal Cys-rich region of mumps virus structural V protein correlates with block of interferon α and γ signal transduction pathway through decrease of STAT-1α. Biochem. Biophys. Res. Commun. **283:**255–259.
36. **Levy, D. E., D. J. Lew, T. Decker, D. S. Kessler, and J. E. Darnell, Jr.** 1990. Synergistic interaction between interferon-alpha and interferon-gamma through induced synthesis of one subunit of the transcription factor ISGF3. EMBO J. **9:**1105–1111.
37. **Li, M., B. Damania, X. Alvarez, V. Ogryzko, K. Ozato, and J. U. Jung.** 2000. Inhibition of p300 histone acetyltransferase by viral interferon regulatory factor. Mol. Cell. Biol. **20:**8254–8263.
38. **Li, M., H. Lee, J. Guo, F. Neipel, B. Fleckenstein, K. Ozato, and J. U. Jung.** 1998. Kaposi's sarcoma-associated herpesvirus viral interferon regulatory factor. J. Virol. **72:**5433–5440.
39. **Lin, R., P. Genin, Y. Mamane, M. Sgarbanti, A. Battistini, W. J. Harrington, Jr., G. N. Barber, and J. Hiscott.** 2001. HHV-8 encoded vIRF-1 represses the interferon antiviral response by blocking IRF-3 recruitment of the CBP/p300 coactivators. Oncogene **20:**800–811.
40. **Luo, Y., H. Yu, and B. M. Peterlin.** 1994. Cellular protein modulates effects of human immunodeficiency virus type I Rev. J. Virol. **68:**3850–3856.
41. **Macrae, A. I., E. J. Usherwood, S. M. Husain, E. Flano, I. J. Kim, D. L. Woodland, A. A. Nash, M. A. Blackman, J. T. Sample, and J. P. Stewart.** 2003. Murid herpesvirus 4 strain 68 M2 protein is a B-cell associated antigen important for latency but not for lymphocytosis. J. Virol. **77:**9700–9709.
42. **Martinez-Guzman, D. A., T. Rickabaugh, T. T. Wu, H. Brown, S. Cole, M. J. Song, L. M. Tong, and R. Sun.** 2003. Transcription program of murine gammaherpesvirus 68. J. Virol. **77:**10488–10503.
43. **Matthews, D. A., and W. C. Russell.** 1998. Adenovirus core protein V interacts with p32—a protein which is associated with both the mitochondria and the nucleus. J. Gen. Virol. **79:**1677–1689.
44. **Mohan, K. V., B. Ghebrehiwet, and C. D. Atreya.** 2002. The N-terminal conserved domain of rubella virus capsid interacts with the C-terminal region of cellular p32 and overexpression of p32 enhances the viral infectivity. Virus Res. **85:**151–161.
45. **Morrison, T. E., A. Mauser, A. Wong, J. P. Ting, and S. C. Kenney.** 2001. Inhibition of IFN-gamma signaling by an Epstein-Barr virus immediate-early protein. Immunity **15:**787–799.
46. **Nash, A. A., B. M. Dutia, J. P. Stewart, and A. J. Davison.** 2001. Natural history of murine gamma-herpesvirus infection. Philos. Trans. R. Soc. Lond. B Biol. Sci. **356:**569–579.
47. **Parisien, J. P., J. F. Lau, J. J. Rodriguez, B. M. Sullivan, A. Moscona, G. D. Parks, R. A. Lamb, and C. M. Harvath.** 2001. The V protein of human parainfluenzavirus 2 antagonizes type I interferon responses by destabilizing signal transducer and activator of transcription 2. Virology **283:**230–239.
48. **Petersen-Mahrt, S. K., C. Estmer, C. Öhrmalm, D. A. Matthews, W. C. Russell, and G. Akusjärvi.** 1999. The splicing factor-associated protein, p32, regulating RNA splicing by inhibiting ASF/SF2 RNA binding and phosphorylation. EMBO J. **18:**1014–1024.
49. **Rajcani, J., D. Blaskovic, J. Svobodova, F. Ciampor, D. Huckova, and D. Stanekova.** 1985. Pathogenesis of acute and persistent murine herpesvirus infection in mice. Acta Virol. **29:**51–60.
50. **Rodriguez, J. J., J. P. Parisien, and C. M. Horvath.** 2002. Nipah virus V protein evades alpha and gamma interferons by preventing STAT1 and STAT2 activation and nuclear accumulation. J. Virol. **76:**11476–11483.
51. **Rodriguez, J. J., L. F. Wang, and C. M. Horvath.** 2003. Hendra virus V protein inhibits interferon signaling by preventing STAT1 and STAT2 nuclear accumulation. J. Virol. **77:**11842–11845.
52. **Schindler, C., X. Y. Fu, T. Improta, R. Aebersold, and J. E. Darnell, Jr.** 1992. Proteins of transcription factor ISGF-3: one gene encodes the 91- and 84-kDa ISGF-3 proteins that are activated by interferon alpha. Proc. Natl. Acad. Sci. USA **89:**7836–7839.
53. **Shuai, K., C. Schindler, V. R. Prezioso, and J. E. Darnell, Jr.** 1992. Activation of transcription by IFN-gamma: tyrosine phosphorylation of a 91-kD DNA binding protein. Science **258:**1808–1812.

54. **Simas, J. P., and S. Efstathiou.** 1998. Murine gammaherpesvirus 68: a model for the study of gammaherpesvirus pathogenesis. Trends Microbiol. **6:**276–282.
55. **Stevenson, P. G., and P. C. Doherty.** 1999. Non-antigen-specific B-cell activation following murine gammaherpesvirus infection is CD4 independent in vitro but CD4 dependent in vivo. J. Virol. **73:**1075–1079.
56. **Stewart, J. P.** 1999. Of mice and men: murine gammaherpesvirus 68 as a model. Epstein-Barr Virus Rep. **6:**31–35.
57. **Stewart, J. P., E. J. Usherwood, A. Ross, H. Dyson, and T. Nash.** 1998. Lung epithelial cells are a major site of murine gammaherpesvirus persistence. J. Exp. Med. **187:**1941–1951.
58. **Stutz, A. M., L. A. Pickart, A. Trifilieff, T. Baumruker, E. Prieschl-Strassmayr, and M. Woisetschlager.** 2003. The Th2 cell cytokines IL-4 and IL-13 regulate found in inflammatory zone 1/resistin-like molecule alpha gene expression by a STAT6 and CCAAT/enhancer-binding protein-dependent mechanism. J. Immunol. **170:**1789–1796.
59. **Sunil-Chandra, N. P., S. Efstathiou, and A. A. Nash.** 1992. Murine gammaherpesvirus 68 established a latent infection in mouse B lymphocytes in vivo. J. Gen. Virol. **77:**3275–3279.
60. **Sunil-Chandra, N. P., S. Efstathiou, and A. A. Nash.** 1992. Virological and pathological features of mice infected with murine gammaherpesvirus 68. J. Gen. Virol. **73:**2347–2356.
61. **Ulane, C. M., and C. M. Horvath.** 2002. Paramyxoviruses SV5 and HPIV2 assemble STAT protein ubiquitin ligase complexes from cellular components. Virology **304:**160–166.
62. **Usherwood, E. J., D. J. Roy, K. Ward, S. L. Surman, B. M. Dutia, M. A. Blackman, J. P. Stewart, and D. L. Woodland.** 2000. Control of gammaherpesvirus latency by latent antigen-specific $CD8^+$ T cells. J. Exp. Med. **192:**943–952.
63. **van Leeuwen, H. C., and P. O'Hare.** 2001. Retargeting of the mitochondrial protein p32/gC1Qr to a cytoplasmic compartment and the cell surface. J. Cell Sci. **114:**2115–2123.
64. **Van Sant, C., R. Hagglund, P. Lopez, and B. Roizman.** 2001. The infected cell protein 0 of herpes simplex virus 1 dynamically interacts with proteasomes, binds and activates the cdc34 E2 ubiquitin-conjugating enzyme, and possesses in vitro E3 ubiquitin ligase activity. Proc. Natl. Acad. Sci. USA **98:**8815–8820.
65. **Van Scoy, S., I. Watakabe, A. R. Krainer, and J. Hearing.** 2000. Human p32: a coactivator for Epstein-Barr virus nuclear antigen-1-mediated transcriptional activation and possible role in viral latent cycle DNA replication. Virology **275:**145–157.
66. **Virgin, H. W., P. I. V. Latreille, P. Wamsley, K. Hallsworth, K. E. Weck, A. J. Dal Canto, and S. H. Speck.** 1997. Complete sequence and genomic analysis of murine gammaherpesvirus 68. J. Virol. **71:**5894–5904.
67. **Virgin, H. W., R. M. Presti, X. Y. Li, C. Liu, and S. H. Speck.** 1999. Three distinct regions of the murine gammaherpesvirus 68 genome are transcriptionally active in latently infective mice. J. Virol. **73:**2321–2332.
68. **Wang, Y. L., J. E. Finan, J. M. Middeldorp, and S. D. Hayward.** 1997. p32/TAP, a cellular protein that interacts with EBNA-1 of Epstein-Barr virus. Virology **236:**18–29.
69. **Weck, K. E., A. J. Dal Canto, J. D. Gould, A. K. O'Guin, K. A. Roth, J. E. Saffitz, S. H. Speck, and H. W. Virgin.** 1997. Murine γ-herpesvirus 68 causes severe large-vessel arteritis in mice lacking interferon-γ responsiveness: a new model for virus-induced vascular disease. Nat. Med. **3:**1346–1353.
70. **Weck, K. E., S. S. Kim, H. W. Virgin IV, and S. H. Speck.** 1999. B cells regulate murine gammaherpesvirus 68 latency. J. Virol. **73:**4651–4661.
71. **Weck, K. E., S. S. Kim, H. W. Virgin IV, and S. H. Speck.** 1999. Macrophages are the major reservoir of latent murine gammaherpesvirus 68 in peritoneal cells. J. Virol. **73:**3273–3283.
72. **Yokota, S., N. Yokosawa, T. Kubota, T. Suzdtani, I. Yoshida, S. Miura, K. Jimbow, and N. Fujii.** 2001. Herpes simplex virus type 1 suppresses the interferon signaling pathway by inhibiting phosphorylation of STATs and janus kinases during an early infection stage. Virology **286:**119–124.
73. **Yu, L., P. M. Loewenstein, Z. Zhang, and M. Green.** 1995. In vitro interaction of the human immunodeficiency virus type I Tat transactivator and the general transcription factor TFIIB with the cellular protein TAP. J. Virol. **69:**3017–3023.